HHS Public Access

Author manuscript

J Biomed Mater Res A. Author manuscript; available in PMC 2015 December 04.

Published in final edited form as:

J Biomed Mater Res A. 2015 February ; 103(2): 451–462. doi:10.1002/jbm.a.35195.

Lubricin: A novel means to decrease bacterial adhesion and proliferation

George E. Aninwene II[1], **Pegah N. Abadian**[1], **Vishnu Ravi**[2], **Erik N. Taylor**[1], **Douglas M. Hall**[3], **Amy Mei**[3], **Gregory D. Jay**[3,4], **Edgar D. Goluch**[1], and **Thomas J. Webster**[1,5]

[1]Department of Chemical Engineering, Northeastern University, Boston, Massachusetts 02115

[2]Albany Medical College, Albany, New York 12208

[3]School of Engineering, Brown University, Providence, Rhode Island 02912

[4]Department of Emergency Medicine, Brown University School of Medicine, Providence, Rhode Island 02912

[5]Center of Excellence for Advanced Materials Research, King Abdulaziz University, Jeddah, Saudi Arabia

Abstract

This study investigated the ability of lubricin (LUB) to prevent bacterial attachment and proliferation on model tissue culture polystyrene surfaces. The findings from this study indicated that LUB was able to reduce the attachment and growth of *Staphylococcus aureus* on tissue culture polystyrene over the course of 24 h by approximately 13.9% compared to a phosphate buffered saline (PBS)-soaked control. LUB also increased *S. aureus* lag time (the period of time between the introduction of bacteria to a new environment and their exponential growth) by approximately 27% compared to a PBS-soaked control. This study also indicated that vitronectin (VTN), a protein homologous to LUB, reduced bacterial *S. aureus* adhesion and growth on tissue culture polystyrene by approximately 11% compared to a PBS-soaked control. VTN also increased the lag time of *S. aureus* by approximately 43%, compared to a PBS-soaked control. Bovine submaxillary mucin was studied because there are similarities between it and the center mucin-like domain of LUB. Results showed that the reduction of *S. aureus* and *Staphylococcus epidermidis* proliferation on mucin coated surfaces was not as substantial as that seen with LUB. In summary, this study provided the first evidence that LUB reduced the initial adhesion and growth of both *S. aureus* and *S. epidermidis* on a model surface to suppress biofilm formation. These reductions in initial bacteria adhesion and proliferation can be beneficial for medical implants and, although requiring more study, can lead to drastically improved patient outcomes.

Keywords

lubricin; biofouling; infection; implant; protein coating; bacterial adhesion; *Staphylococcus aureus*; *Staphylococcus epidermidis*; kinetic bacterial growth modeling

Correspondence to: T. J. Webster; th.webster@neu.edu.

INTRODUCTION

Infection after the implantation of a medical device is a persistent problem in medicine. The success of medical devices (such as heart valves, endotracheal tubes, pacemakers, orthopedic implants, intraocular lenses, central venous catheters, and orthopedic joint prosthetics) are threatened by the attachment and proliferation of bacteria on their surfaces after implantation.[1,2] Postsurgical infection can be costly, result in additional morbidity to the patient, and possibly require revision surgery. For example, endophthalmitis is a serious intraocular infection that can result as a complication of intraocular surgery.[3] Endophthalmitis can cost approximately $12,580 (US) in total ophthalmic medical care claims per patient treated and can lead to severe permanent visual impairment or a complete loss of the infected eye.[3–5] In addition, central intravenous catheters (CVCs) can cause bloodstream infections (BSIs) in about 4–5 cases out of every 1000 CVC devices inserted.[6–8] The estimated annual cost of caring for patients with CVC-associated BSIs ranges from $296 million to $2.3 billion (USD).[9] It is clear that infections in postsurgery and critical care patients are costly and potentially life threatening.

Once bacteria attach to a substrate, their functions change and the host's defenses are incapable of combating the subsequent colonization and biofilm formation.[10] Biofilms are the hydrated polymeric matrix that bacteria form once they aggregate on a surface, protecting the bacteria through inherent resistance to an immune response and antimicrobial agents.[10] A study by Kluytmans et al.[11] reported that disruptions of hydrophobic surface interactions may prevent initial bacterial binding and inhibit bacterial colonization. If the bacteria are not able to colonize a surface and form a biofilm, it will be much easier for the immune system to clear these bacteria before they cause an infection.

Staphylococcus aureus and *Staphylococcus epidermidis* are two major opportunistic pathogenic, biofilm producing, bacteria that colonize a large portion of the human population.[12] Both are major culprits of biofouling and postsurgical infections. Multiple strains of antibiotic-resistant *S. epidermidis* and *S. aureus* have been linked to a growing number of hospital acquired and postoperative infections.[1,12,13] *S. epidermidis* is primarily located throughout the cutaneous ecosystem, while *S. aureus* is carried primarily on mucosal surfaces.[12]

S. aureus is regarded as one of the leading causes of aggressive, persistent postsurgical infections due to acquired resistance to antibiotics and its ability to form drug-resistant biofilms.[14] Lowy[15] states that "Humans are a natural reservoir of S. aureus" and goes on to say that 30–50% of adults are colonized, with 10–20% persistently colonized. *S. aureus* infections cause a range of acute and pyogenic infections, including abscesses, bacteremia, central nervous system infections, endocarditis, osteomyelitis, pneumonia, urinary tract infections, chronic lung infections associated with cystic fibrosis, and several syndromes caused by exotoxins and enterotoxins, including food poisoning and scalded skin and toxic shock syndromes.[12] The overuse of methicillin and other semisynthetic penicillins in the late 1960s led to the emergence of methicillin-resistant *S. aureus*. In 1997, approximately 60% of *S. aureus* isolated from patients were resistant to methicillin.[12] Additionally, new

antibiotic-resistant bacteria strains continue to emerge that are resilient to even last resort antibiotics, such as vancomycin.[16]

Although it is a less aggressive of a pathogen than *S. aureus*, *S. epidermidis* is a major nosocomial pathogen which is primarily associated with infections of implanted medical devices.[12,17] The overuse of methicillin and other semisynthetic penicillins in the late 1960s also led to the emergence of methicillin-resistant *S. epidermidis* (MRSE).[12] Once again, new antibiotic-resistant strains of these bacteria continue to emerge. One effective treatment against multidrug-resistant staphylococci, including MRSE, was the glycopeptide antibiotic vancomycin; however, resistance has developed to this treatment as well.[12] *S. epidermidis* biofilms comparatively grow into thicker and highly robust biofilms in particular through the production of intracellular polysaccharide adhesins, which protects the bacterial colonies from the antibiotic treatments and immune response.[18,19]

Along this line, there is promise in modifying implant surfaces to reduce the occurrence of these postoperativeinfection based complications. Prior studies have been performed using antibiotic drug coatings on medical implants to prevent biofouling; however, as mentioned, a sustained use of antibiotics can lead to pathogenic bacteria developing resistance to the antibacterial treatment.[20] There is a need for surface treatments which will prevent bacterial attachment without promoting the development of additional strains of antibiotic-resistant bacteria. This study sought to investigate a naturally occurring antiadhesive alternative to antibiotic surface treatments. This study proposes, for the first time, the use of the glycoprotein lubricin (LUB) as an antibiofouling surface coating agent.

LUB is a glycoprotein found in the synovial fluid that plays a major role in its lubricating and antiadhesive properties.[21] LUB has a mucin-like center domain and globular N-terminal and C-terminal domains (Figure 1).[25] The purpose of this *in vitro* study was to determine: (1) LUB's ability to prevent bacterial adhesion and proliferation under tissue culture conditions on a model tissue culture surface (polystyrene), (2) its ability to serve as an effective nonimmune opsonification agent for resisting bacteria colonization, and (3) to provide evidence that LUB is a viable means to prevent bacteria adhesion, proliferation, and biofilm production under flow conditions. Bovine submaxillary mucin (BSM) was used as a control due to the structural similarities between mucin and the center domain of LUB. The main differences between mucin and LUB is that mucin lacks the globular hydrophobic end domains found in LUB and mucin does not display LUB's boundary lubricating properties.[26] Vitronectin (VTN) was also used as a control because it is a homologous protein to LUB. Although LUB and VTN have a 60% sequence similarity, VTN lacks the center mucin-like domain found in LUB.[27]

EXPERIMENTAL DETAILS

Substrate

Standard tissue culture polystyrene was used as the polymer substrate. Sterile tissue culture polystyrene plates were obtained from Becton, Dickinson and Company. The LUB used in these trials was extracted under sterile conditions from bovine synovial fluid obtained from Pel-Freez Arkansas, LLC. The sterile extraction of LUB from synovial was described fully

by Jay et al., but in short it involves extraction of LUB from bovine synovial fluid through a hyaluronate digestion, followed by anion exchange chromatography, and an affinity chromatography to purify and concentrate the protein.

Protein preparation

Aliquots of bovine VTN of 50 μg (Sigma–Aldrich, St. Louis, MO) were dissolved in 1 mL of sterile phosphate buffered saline (PBS). LUB and BSM (Sigma–Aldrich) were used at a concentration of 200 μg/mL. Prior to use, both BSM and VTN solutions were filtered through low protein binding sterile filters with a pore diameter of 0.2 μm (Corning). Each protein solution of 50 μL was dried on the well surface overnight at room temperature, under sterile conditions.

Bacteria surface adhesion and proliferation study

S. aureus—*S. aureus* obtained from the American Type Culture Collection (25923) was cultured in tryptic soy broth (TSB; Sigma Aldrich) for 18 h to reach stationary phase, then diluted to a density of 1×10^7 bacteria/mL (as estimated by the McFarland scale which corresponded to an optical density of 0.52 at 562 nm and then further diluting at a ratio of 1:90).[1] The 96-well polystyrene tissue culture plates were treated with LUB, BSM, or VTN. LUB and BSM were used in the crystal violet end point trials, while LUB, BSM, and VTN were used in the 24-h optical density trials. Bacterial solutions were seeded into the treated 96-well culture plates and incubated for 15 min in a stationary incubator maintained at 37°C. After 15 min, the bacterial solution was removed, the plates were rinsed three times with sterile PBS, and the wells were filled with 200 μL of fresh TSB.

For crystal violet trials, plates were incubated for 24 h, after which crystal violet was used to determine the quantity of bacterial biofilm formed. For this, plates were rinsed once with PBS, followed by the addition of 175 μL of a crystal violet solution (Sigma) into each well and then allowed to act for 15 min to stain the biofilm. Solutions were then removed and the plates were again rinsed three times with PBS and plates were allowed to dry at room temperature. Once dry, 200 μL of ethanol were added and after 15 min optical density readings were read at 562 nm with a Spectramax 340PC spectrophotometer (Molecular Devices).

For 24-h optical density trials, after the initial bacterial seeding and rinsing steps, the Spectramax 340PC spectrophotometer was used to determine optical density measurements, at 562 nm, every 4 min for 24 h while maintaining the temperature at 37°C. Comparisons were made between the PBS coated samples and the protein coated samples and the percent difference was calculated for every data point over the course of the experiment.

S. epidermidis—The 96-well polystyrene tissue culture plates were treated in a manner similar to the *S. aureus* trials. However, the initial seeding volume of the bacterial solution was 50 μL of *S. epidermidis* (American Type Culture Collection (35984)) diluted in the same manner mentioned above (approximately 1×10^7 bacteria/mL). After 15 min, the bacterial solution was removed, the plates were rinsed three times with sterile PBS, and the wells were filled with 200 lL of fresh TSB. Crystal violet end point trials and 24 h optical

density trials were done in the same manner as described above. Comparisons were done between the PBS coated samples and the protein coated samples and the percent difference was calculated for every data point over the course of the experiment.

Modeling—The ability of LUB to inhibit bacterial proliferation was quantified in this study by determining the effect that LUB and protein subregions of LUB (mucin and VTN) have on the growth curve of each bacterium. This curve is generally separated into several phases. The first is the *lag phase* during which the bacteria are adapting to the conditions of their environment and not dividing. The lag time (λ) is the length of this phase. Then, there is an *exponential phase* during which the bacteria are dividing at a constant rate, leading to exponential growth. In this phase, if the natural logarithm of the number of organisms is plotted against time, a straight line will result. The slope of this line is the maximum specific growth rate (μ_m). Depletion of essential nutrients and/or formation of toxins and inhibitory products causes the bacteria to enter the *stationary phase* during which the growth and death rate are equal.[29] The ratio of the number of organisms in this equilibrium state to initial number of organisms is the upper asymptote (A).

The three values (λ, μ_m, and A) were determined here by fitting the bacterial growth data to two sigmoid growth functions: the logistic function and the Gompertz function. These are both mathematical models of a time series where the growth at the beginning and end of the period of time is the smallest. The logistic function is symmetrical about its inflection point, while the Gompertz function approaches its upper asymptote more slowly than its lower asymptote.

The growth data (optical density vs. time) obtained from these bacterial trials were fit to modified forms of the logistic model [Eq. (1)] and the Gompertz model [Eq. (2)] using MATLAB R2013a.

$$\ln\left(\frac{OD_t}{OD_0}\right) = \frac{A}{\left\{1+e^{\left[\frac{4\mu_m}{A}(\lambda-t)+2\right]}\right\}} \quad (1)$$

$$\ln\left(\frac{OD_t}{OD_0}\right) = Ae^{-e^{\frac{\mu_m+e}{A}(\lambda-t)+1}} \quad (2)$$

The model equations used were modified from their generic forms to contain coefficients for the three bacterial growth parameters lag time (λ), maximum specific growth rate (μ_m), and the asymptote of the stationary phase (A) by deriving formulas to represent the mathematical parameters in terms of the bacterial growth parameters.[30] OD_t is the optical density at time t and OD_0 is the optical density at the start of the experiment. The goodness-of-fit was determined using R^2 and the sum of squares for error (SSE). The models with the best fit were used to determine the value of the three parameters for each combination of bacteria and protein.

Surface plasmon resonance imaging biofilm adhesion study—Surface plasmon resonance imaging (SPRi), performed in a HORIBA Scientific SPRi-Lab+ device (HORIBA

Scientific), provided label-free quantitative and qualitative information about events occurring on and near the surface (~200 nm) over a relatively large area (~1 cm).[31–3] SPRi instruments operate by light transmission through a high refractive index glass prism onto a gold surface, followed by subsequent detection events that manifest themselves as changes in the intensity of reflected light that exits the prism, which is measured using a charge coupled device (CCD) camera.[32,33] Light of a certain wavelength is projected onto the metal surface through the glass prism. At the surface interface the light is converted into surface plasmon polaritons (SPPs). Attachment events on the surface of the metal result in changes in the refractive index, resulting in the loss of SPP generation at the specific attachment site. Thus, if there is an attachment at the surface of the metal, the light will be reflected back and detected by a CCD camera and bright spots will appear on the image.[32]

A glass prism was purchased with a 50-nm layer of bare gold on top (SPRi-Biochip; HORIBA Scientific). Polydimethyl-siloxane (PDMS; Sylgard 184 PDMS kit; Dow Chemical) was used to create a 300 μL growth chamber over the surface of the prism. Prior to trials, the prism and flow chamber were cleaned and sterilized using 70% EtOH and rinsed with deionized water. Once the flow chamber and prism were cleaned and aligned, approximately 5 μL of each protein solution were streaked onto the growth chamber and allowed to dry for 3 h at room temperature under sterile conditions. For these trials, both LUB and BSM were used at a concentration of 200 μg/mL. Once dry, the growth chamber was seeded with 300 μL of *S. aureus* using 6 mL of Difco Luria Bertani Broth (LB) Growth Media (Miller) inoculated with *S. aureus* incubated for 18 h at 37°C and then diluted 1:100 in LB, yielding approximately 5×0^6 bacteria/mL. Thereafter, the growth chamber was inserted into the SPRi device and a flow rate of LB growth media was maintained at 10 μL/min (Figure 2). The trial was run for one day, and the Horiba SPRi apparatus was set to take measurements and images every 3 min. The changes in reflectivity of the surface indicated the adherence of bacteria and growth of a biofilm on the surface.[1,3] The numerical values were paired with the visual images obtained during the trials to measure the relative quantity of biofilm formed on the gold surface of the prism in the coated and uncoated regions.

Contact angles

Contact angle measurements were made using a Krüss Easy Drop contact angle instrument (Hamburg, Germany) connected to an image analysis program (Drop Shape Analysis, Version 1.8). The tissue culture polystyrene samples were dried overnight under vacuum after coating. The Krüss Easy Drop apparatus was used to measure the contact angles that resulted when a 10 μL drop of each test liquid (H_2O, glycerol, or ethylene glycol) was dispensed onto the surface of the sample. The Krüss Trackman software was used to record the contact angle after the drop was placed on the surface within 30 s of the droplet being dispensed. All readings were taken at ambient room temperature.

Statistical analysis

All of the above trials were performed with a minimum of three replicates each. The standard error of the mean was used to describe variance about the mean. Statistical analysis of numerical data in this study was completed using an unpaired *t*-test assuming unequal

variances. Statistical significance was considered at $p < 0.05$. For the bacteria surface adhesion and proliferation study, a 95% confidence interval was determined at each time point and was used as an additional method to ensure statistical differences between experimental and control trials.

RESULTS

Bacteria surface adhesion and proliferation study

S. aureus—The polystyrene bacteria trials showed that treatment with 200 μg/mL LUB reduced *S. aureus* optical density when compared with the controls [Fig. 3(B)]. Over the course of the experiment, the protein-coated samples showed a significant decrease in growth when compared to the PBS coated samples at approximately 3.9 h (near the start of the exponential growth phase) as indicated by the growth curve. This trend of a decrease at the start of the exponential phase was seen with samples coated with LUB, VTN, and BSM. Mathematical modeling of the data showed that all three proteins increased the length of the lag phase compared to controls (Fig. 4).

As seen in Figure 3(B), between the period of 3.9 and 5.1 h, there was a significant decrease ($p < 0.05$) in the LUB growth curve versus the control PBS growth curve. After 9.6 h, there was a 13.87% difference between the LUB coated samples and the PBS-coated samples ($p < 0.05$). This indicated that the LUB suppressed the attachment and proliferation of *S. aureus* during the exponential phase of bacteria growth, and reduced the overall amount of bacterial proliferation once the bacteria reached the stationary phase. The mathematical model showed that there was a 27% (51.6 min) increase in lag time (Fig. 4), a 13% reduction in the ratio of equilibrium number of bacteria in the stationary phase to the initial number of bacteria, and a decrease in the maximum specific growth rate.

In the VTN *S. aureus* trial, the first period of significant reduction in the bacterial growth curve was between 3.9 and 5.6 h [Fig. 3(C), $p < 0.05$]. After 10.9 h, the VTN growth curve continued to show a significant difference from the control PBS-soaked samples. The difference of 13 and 14.4 h was less significant [Fig. 3(C), $p < 0.058$]. However, after 14.4 h the difference from the control PBS-soaked samples remained very significant [Fig. 3(C), $p < 0.05$]. At the end of 24 h there was a 10.96% difference between the VTN-soaked sample and the control PBS-soaked samples. Again, this indicated that the protein disrupted the start of the exponential growth phase as well as the stationary phase. The mathematical model showed an increase in lag time of 43% [82.2 min; Fig. 4(A)], a 13% reduction in the ratio of equilibrium number of bacteria in the stationary phase to the initial number of bacteria and an increase in the maximum specific growth rate.

In the case of BSM, there was a significant reduction in bacterial proliferation between 4.13 and 4.9 h [Fig. 3(D), $p < 0.05$]. While some disruption of the exponential growth phase was observed, there was no prolonged effect of BSM on *S. aureus* in the stationary phase. However, the crystal violet trials showed that while the LUB resulted in a minor reduction in biofilm production, the BSM coated samples showed a 58% reduction in adherent biofilms when compared to the PBS coated samples [Fig. 3(A)]. The difference in the crystal violet results indicate that although BSM may not reduce initial bacteria adhesion and proliferation

as well as LUB, biofilms grown on BSM coated surfaces appeared to be drastically less than those grown on LUB coated or control PBS coated surfaces. The mathematical model showed a 29% (55.4 min) increase in lag time (Fig. 4), a significant decrease in maximum specific growth rate, and no significant change in asymptote between BSM and the control PBS-soaked samples.

S. epidermidis—The 24-h polystyrene bacterial growth trials showed that treatment with 200 μg/mL LUB resulted in a significant retardation of the *S. epidermidis* growth curve when compared with the control [Fig. 5(B)]. Over the course of the experiment, the LUB and BSM coated samples showed a significant decrease at approximately 6.2 h, near the start of the exponential growth phase, as indicated by the growth curve. Mathematical modeling showed that treatment with LUB and BSM resulted in an increase in lag time, whereas treatment with VTN resulted in a small decrease in lag time (Table II, Fig. 6).

As seen in Figure 5(B), between the period of 6.2 and 12.2 h there was a significant depression in the LUB growth curve versus the control PBS growth curve ($p<0.05$). This indicated that LUB initially suppressed attachment and retarded the initial proliferation of *S. epidermidis*. The crystal violet trials showed that the LUB coated samples caused a minor reduction in biofilm production when compared to the PBS coated samples [Fig. 5(A)]. The mathematical model showed a 36% (105.7 min) increase in lag time (Fig. 6), no significant difference in the asymptote, and a slight increase in maximum specific growth rate.

VTN did not appear to significantly decrease *S. epidermidis* proliferation [Fig. 5(D)]. From the mathematical model, no significant difference in the lag time was observed between the VTN coated samples and the PBS coated samples. However, there was a 3% decrease in asymptote, and a significant decrease in maximum specific growth rate between the VTN coated samples and the PBS coated samples.

In the case of BSM, there was a significant reduction in bacterial proliferation between 6.3 and 9.6 h [Fig. 5(C), $p<0.05$]. While some disruption of the exponential growth phase was observed there was no prolonged effect of BSM, indicating a significant *S. epidermidis* reduction once the stationary phase was reached. Crystal violet trials showed that BSM coated samples had a 15.5% reduction in adherent biofilms when compared to PBS coated samples [Fig. 5(A)]. The mathematical model showed a 30% increase in lag time (Fig. 6), no significant reduction in asymptote, and no significant reduction in maximum specific growth rate.

Modeling—The modified Gompertz and Logistic models both fit the bacterial growth data very closely. The modified Gompertz model had a slightly better fit for 8 of the 10 data sets based on the R^2 and SSE (Figs. 7 and 8). Therefore, the Gompertz model was used to compare the growth parameters between different protein treatments of each bacterium. A summary of results derived from the models can be found in Tables I and II.

Surface plasmon resonance imaging—LUB coated areas of the gold surface were almost completely devoid of *S. aureus* biofilm production, while mucin-coated areas initially resisted biofilm production (Fig. 9). At the end of the trials, LUB showed over a

90% clearance when compared to bare gold, while mucin only resulted in approximately 7% reduction in biofilm adherence and proliferation compared to bare gold (Fig. 10).

Contact angles

In our trials, all samples that were soaked in PBS showed rapid and complete wetting and the initial contact angle could not be measured with our equipment. Since LUB was dissolved in PBS, all the tissue culture polystyrene samples soaked in LUB solutions showed complete wetting. Table III shows the mean values of the contact angle measurements for uncoated tissue culture-treated polystyrene.

DISCUSSION

Lubricin

LUB is an amphiphilic glycoprotein that is found in synovial fluid; the molecular weight of LUB is approximately 240 kDa and the molecular structure is similar to an extended flexible rod with a length of approximately 200 nm and a width of approximately 1–2 nm[34,36] (Fig. 1). The half-life of this molecule is approximately 6 days when bound to cartilage.[37] In humans, the concentration of LUB ranges from 52 to 350 μg/mL in normal joints examined postmortem and 276 to 762 μg/mL in the synovial fluid obtained from patients undergoing arthrocentesis procedures.[38]

The abundance of negatively charged and highly hydrated sugars in the center mucin-like domain of LUB contribute to its boundary lubrication properties as a result of strong repulsion through steric and hydration forces.[22] On hydrophobic surfaces, the globular tail ends or the hydrophobic motifs in the mucin domain will orient themselves toward and adsorb to the substrate, while on hydrophilic surfaces, the mucin-like domain will orient toward, and adsorb to the substrate, as illustrated in Figure 1.[21,22] Thus, LUB coating imparts a negatively charged hydrophilic nature on to the coated surface.

The sugars in the central mucin-like domain of LUB are O-linked glycosylations and have been studied by Jay et al.[39] Sugars in the central mucin-like domain have been characterized as disaccharide β(1–3)Gal-GalNAc and trisaccharide β(1–3)Gal-Gal-NAc-NeuAc moieties.[39] The densely packed sialic acid residues and sulfate groups are responsible for the negative charge as well as the hydrophilic nature of the central domain of LUB.[40]

LUB's amino acid sequence has significant similarities to the adhesive protein VTN.[27] Both proteins contain somatomedin B (SMB) and hemopexin-like (PEX) domains and there is approximately a 60% sequence similarity between both proteins.[27] In VTN, SMB and PEX sequences are known to regulate the complement and coagulation systems, mediate extracellular matrix attachment, and promote cell attachment and proliferation.[27] The PEX and SMB domains are found in the globular tails of LUB as seen in Figure 1.[24,27,41]

Previous studies have shown that in addition to providing boundary layer lubrication, LUB plays a role in reducing or preventing undesirable cellular attachment. Rhee et al.[27] showed that LUB was able to reduce synovial cell overgrowth within joints and Noyori and Jasin[42] indicated that LUB may be responsible for the inability of fibroblasts to adhere to healthy

cartilage. However, previous studies from other research groups have not investigated the antibacterial or bacteriostatic properties of LUB. This study showed, for the first time, that LUB significantly reduced the initial attachment and proliferation of bacteria. The most striking change was the significant increase in the length of the lag phase (36% for *S. epidermidis* and 27% for *S. aureus*) indicating that LUB made it more difficult for the bacteria to adapt to the surface and begin to grow. The SPRi trials definitively displayed activity by LUB to stop biofilms under flow, simulating conditions that would be expected in the body (i.e., vascular flow or other fluid exchange). Under flow conditions, a LUB coating dried onto a surface and was able to impede over 90% of *S. aureus* biofilm production.

Mucin—As previously mentioned, LUB has a central mucin-like domain. Mucins are large glycoproteins that are the major components in mucus that cover the luminal surfaces of epithelial organs.[43] Additionally, mucins are found in mucus which forms a physical barrier between plasma membranes and the extracellular environment.[43] Their structure can be described as a threadlike peptide backbone, with densely packed carbohydrate side chains.[43] Mucins have unique properties as surfactants. They adsorb to hydrophobic surfaces via surface-protein interactions while clinging to water molecules through their hydrophilic oligosaccharide clusters (Fig. 1).[43]

Secretory mucins typically have a very high molecular mass and contain hundreds of O-linked saccharide side chains, constituting between 50 and 90% of their molecular weight.[40,44] The oligosaccharide side chains are about 5–15 monomers long and are O-linked to the serine and threonine residues of the protein core with a sufficiently high density that steric interactions force them to stretch away from the central protein core in a “bottlebrush” configuration.[40] These oligosaccharide side chains are most commonly composed of *N*-acetyl glucosamine, *N*-acetyl galactosamine, galactose, fucose, and sialic acid, and other carbohydrate residues have also been reported.[40] Sialic acid residues are negatively charged and work in concert with sulfate groups to give mucins a net negative charge.[40] Due to their hydrophilic (glycosylated) and hydrophobic (unglycosylated) domains (i.e., an amphiphilic, block-copolymer structure), mucins are able to adhere strongly to a wide range of surfaces by hydrogen bonding, hydrophobic interactions, and by electrostatic interactions.[40] Mucins can vary in size and length due to differing numbers of tandem repeats in the central domain. Even with the same type of mucin, the number of tandem repeats can differ from individual to individual.[45] Work by Shi et al.[43] indicated that mucin surface coatings could decrease bacterial adhesion of *S. aureus* and *S. epidermidis* by reducing the hydrophobic binding forces and by providing a barrier which prevents the bacteria from making close contact with the surfaces. That study showed that when a 1 mg/mL BSM solution was used to coat poly-methyl-methacrylate and polystyrene over a 90% reduction in bacterial adhesion was seen when compared to the uncoated control.[43] The literature indicates their negatively charged glycosylated regions may be responsible for this effect, and noted a relationship between higher mucin concentration on the surface, lower hydrophobicity, and lower bacterial adhesion.[43] However, the study by Shi et al. did not investigate the effects this protein had on bacterial adhesion on the surface past 3 h, nor did it examine the effect this protein coating had on the growth curve of the bacteria. In this

study, our group more thoroughly investigated the protein effect on the growth curve by gathering 24-h kinetic data of bacterial growth on mucin-coated surfaces.

Vitronectin—As stated previously there is approximately 60% sequence similarity between LUB and VTN.[27] VTN is a glycoprotein found in the blood and extracellular matrix.[46] VTN is known as “serum spreading factor” and inhibitor of the membrane attack complex of the complement immunoresponse.[46] The molecular weight of human VTN is 75 kDa. It contains three glycosylation sites and its carbohydrate moieties contributes to approximately 30% of its molecular mass.[46] VTN is also a multifunctional protein, and it is highly homologous to LUB. The main difference between VTN and LUB is that VTN lacks a mucin-like central domain.

Bacteria

Surface interactions—Hydrophobic adsorption has been shown to be an important mechanism in the physical interactions of *S. aureus*.[43] Previous studies have shown that bacteria surfaces are negatively charged, and that *S. aureus* has a high relative surface charge and high hydrophobicity.[43] Strong interactions take place between the membrane lipids of bacteria and hydrophobic surfaces.[43] Shi et al.[43] state that the degree of hydrophobicity will determine how well bacteria will adhere to a surface and how extensively they will proliferate. Thus, it follows that reducing the hydrophobicity and applying a negatively charged coating to a surface could result in surfaces that are less prone to bacterial adhesion.

In order to adhere to a surface, bacteria need to establish firm interactions to prevent their rapid elimination by physicochemical mechanisms.[11] Bacterial adherence may be nonspecifically mediated by physicochemical forces, such as hydrophobic interactions.[11] Disruptions of these hydrophobic interactions may prevent bacterial binding and lead to a prevention of bacterial colonization. If the bacteria are not able to colonize a surface and form a biofilm, it will be much easier for the immune system to clear these bacteria before they cause an infection. This study shows that LUB inhibits bacterial colonization of surfaces by blocking bacteria interactions with the surface using the biologically derive protein LUB. This study proposes that the negative charge of LUB’s central mucin domain repels the bacteria, and that the protein coating of the LUB blocked other surface proteins from interacting with the surface, further preventing the cells from adhering. Future studies will be needed to confirm this mechanism of repulsion.

CONCLUSIONS

Trials with LUB on polystyrene show that at a surface coating from a working concentration of 200 μg/mL, LUB is able to reduce *S. aureus* adhesion and growth by approximately 13.9% over 24 h and that with a coating concentration of 50 μg/mL, VTN was able to reduce bacterial adhesion and proliferation by approximately 11% over 24 h. Trials with *S. epidermidis* showed that LUB and BSM were able to significantly retard the growth process and delay the start of the exponential growth phases as well. BSM trials indicated that the mucin domain of LUB may provide the mechanism of LUB’s bacteriostatic nature.

Additionally, the crystal violet trials indicated that the mucin domain played a major role in retarding bacterial adhesion and biofilm formation.

Mathematical modeling showed that LUB significantly increased the length of the lag phase of *S. aureus* by 27% and *S. epidermidis* by 36%. These results suggested that LUB makes it more difficult for bacteria to adapt to their environment, and as a result it took longer for the bacteria to enter the phase of exponential growth. This is significant because a longer lag phase will allow more time for the immune system to recognize and clear bacteria either before they start to divide or in the early stages of the exponential growth phase. It will also allow more time for antimicrobial treatments to work, before a persistent infection can occur. Since this study used far greater concentrations of bacteria than are normally found in a physiological environment, it is expected that these effects would much greater *in vivo*.

The SPRi allowed for a better view of bacterial adhesion and biofilm production under flow conditions. These trials showed that LUB may act as a quick and effective method to coat medical implants and used in flow systems such as hemodialysis devices to prevent the accumulation of biofilm and reduce the chances of related blood born infections.

In summary, because of LUB's ability to reduce bacterial attachment and proliferation using only a low concentration of protein and a very simple drying technique for surface coating, LUB shows promise as an antibiofouling agent and bacteriostatic coating. Thus, LUB should be further studied as a means to prevent bacterial infections without risking the development of additional drug-resistant bacteria strains.

Acknowledgments

Special thanks to Evan Smith, Ling Zang, Kimberly Waller, Jara Crear, Justin Seil, and Megan Creighton for aid in experimental design and data analysis.

Contract grant sponsor: Northeastern University, the Hermann Foundation, NIGMS; contract grant numbers: R25GM083270 and R25GM083270-S1

Contract grant sponsor: NSF GK-12 fellowship; contract grant number: 0638688

References

1. Puckett SD, Taylor E, Raimondo T, Webster TJ. The relationship between the nanostructure of titanium surfaces and bacterial attachment. Biomaterials. 2010; 31:706–713. [PubMed: 19879645]
2. Weber DJ, Hoffman KL, Thoft RA, Baker AS. Endophthalmitis following intraocular lens implantation: Report of 30 cases and review of the literature. Rev Infect Dis. 1986; 8:12–20. [PubMed: 3513284]
3. Taban M, Behrens A, Newcomb RL, Nobe MY, Saedi G, Sweet PM, McDonnell PJ. Acute endophthalmitis following cataract surgery: A systematic review of the literature. Arch Ophthalmol. 2005; 123:613–620. [PubMed: 15883279]
4. Sharifi E, Porco TC, Naseri A. Cost-Effectiveness analysis of intracameral cefuroxime use for prophylaxis of endophthalmitis after cataract surgery. Ophthalmology. 2009; 116:1887–1896.e1. [PubMed: 19560825]
5. Schmier JK, Halpern MT, Covert DW, Lau EC, Robin AL. Evaluation of medicare costs of endophthalmitis among patients after cataract surgery. Ophthalmology. 2007; 114:1094–1099. [PubMed: 17320963]

6. Taylor E, Webster TJ. Reducing infections through nanotechnology and nanoparticles. Int J Nanomed. 2011; 6:1463–1473.
7. System Arft N. National Nosocomial Infections Surveillance (NNIS) System Report, data summary from January 1992 through June 2004, issued October 2004. Am J Infect Control. 2004; 32:470–485. [PubMed: 15573054]
8. O'Grady NP, Alexander M, Dellinger EP, Gerberding JL, Heard SO, Maki DG, Masur H, McCormick RD, Mermel LA, Pearson ML, Raad II, Randolph A, Weinstein RA. Guidelines for the prevention of intravascular catheter-related infections. Centers for Disease Control and Prevention. MMWR Recomm Rep. 2002; 51:1–29. [PubMed: 12233868]
9. Mermel LA. Prevention of intravascular catheter-related infections. Ann Intern Med. 2000; 132:391–402. [PubMed: 10691590]
10. Costerton JW, Stewart PS, Greenberg EP. Bacterial biofilms: A common cause of persistent infections. Science. 1999; 284:1318–1322. [PubMed: 10334980]
11. Kluytmans J, van Belkum A, Verbrugh H. Nasal carriage of *Staphylococcus aureus*: Epidemiology, #underlying |mechanisms, and associated risks. Clin Microbiol Rev. 1997; 10:505–520. [PubMed: 9227864]
12. Gill SR, Fouts DE, Archer GL, Mongodin EF, DeBoy RT, Ravel J, Paulsen IT, Kolonay JF, Brinkac L, Beanan M, Dodson RJ, Daugherty SC, Madupu R, Angiuoli SV, Durkin AS, Haft DH, Vamathevan J, Khouri H, Utterback T, Lee C, Dimitrov G, Jiang L, Qin H, Weidman J, Tran K, Kang K, Hance IR, Nelson KE, Fraser CM. Insights on evolution of virulence and resistance from the complete genome analysis of an early methicillin-resistant *Staphylococcus aureus* strain and a biofilm-producing methicillin-resistant *Staphylococcus epidermidis* strain. J Bacteriol. 2005; 187:2426–2438. [PubMed: 15774886]
13. Rubin RJ, Harrington CA, Poon A, Dietrich K, Greene JA, Moiduddin A. The economic impact of *Staphylococcus aureus* infection in New York City hospitals. Emerg Infect Dis. 1999; 5:9–17. [PubMed: 10081667]
14. Suci PA, Varpness Z, Gillitzer E, Douglas T, Young M. Targeting and photodynamic killing of a microbial pathogen using protein cage architectures functionalized with a photosensitizer. Langmuir. 2007; 23:12280–12286. [PubMed: 17949022]
15. Lowy FD. *Staphylococcus aureus* infections. N Engl J Med. 1998; 339:520–532. [PubMed: 9709046]
16. Appelbaum PC. The emergence of vancomycin-intermediate and vancomycin-resistant *Staphylococcus aureus*. Clin Microbiol Infect. 2006; 12:16–23. [PubMed: 16445720]
17. O'Gara JP, Humphreys H. *Staphylococcus epidermidis* biofilms: Importance and implications. J Med Microbiol. 2001; 50:582–587. [PubMed: 11444767]
18. Fey PD, Olson ME. Current concepts in biofilm formation of *Staphylococcus epidermidis*. Future Microbiol. 2010; 5:917–933. [PubMed: 20521936]
19. Rohde H, Burandt EC, Siemssen N, Frommelt L, Burdelski C, Wurster S, Scherpe S, Davies AP, Harris LG, Horstkotte MA, Knobloch JK, Ragunath C, Kaplan JB, Mack D. Polysaccharide intercellular adhesin or protein factors in biofilm accumulation of *Staphylococcus epidermidis* and *Staphylococcus aureus* isolated from prosthetic hip and knee joint infections. Biomaterials. 2007; 28:1711–1720. [PubMed: 17187854]
20. Harding JL, Reynolds MM. Combating medical device fouling. Trends Biotechnol. 2014; 32:140–146. [PubMed: 24438709]
21. Zappone B, Ruths M, Greene GW, Jay GD, Israelachvili JN. Adsorption, lubrication, and wear of lubricin on model surfaces: Polymer brush-like behavior of a glycoprotein. Biophys J. 2007; 92:1693–1708. [PubMed: 17142292]
22. Chang DP, Abu-Lail NI, Guilak F, Jay GD, Zauscher S. Conformational mechanics, adsorption, and normal force interactions of lubricin and hyaluronic acid on model surfaces. Langmuir. 2008; 24:1183–1193. [PubMed: 18181652]
23. Jones ARC, Gleghorn JP, Hughes CE, Fitz LJ, Zollner R, Wainwright SD, Caterson B, Morris EA, Bonassar LJ, Flannery CR. Binding and localization of recombinant lubricin to articular cartilage surfaces. J Orthopaedic Res. 2007; 25:283–292.

24. Zappone B, Greene GW, Oroudjev E, Jay GD, Israelachvili JN. Molecular aspects of boundary lubrication by human lubricin: Effect of disulfide bonds and enzymatic digestion. Langmuir. 2007; 24:1495–1508. [PubMed: 18067335]
25. Jay GD, Torres JR, Warman ML, Laderer MC, Breuer KS. The role of lubricin in the mechanical behavior of synovial fluid. Proc Natl Acad Sci USA. 2007; 104:6194–6199. [PubMed: 17404241]
26. Jay GD, Hong B-S. Characterization of a bovine synovial fluid lubricating factor. II. Comparison with purified ocular and salivary mucin. Connect Tissue Res. 1992; 28:89–98. [PubMed: 1628492]
27. Rhee DK, Marcelino J, Baker M, Gong Y, Smits P, Lefebvre Vr, Jay GD, Stewart M, Wang H, Warman ML, Carpten JD. The secreted glycoprotein lubricin protects cartilage surfaces and inhibits synovial cell overgrowth. J Clin Invest. 2005; 115:622–631. [PubMed: 15719068]
28. Jay GD, Haberstroh K, Cha C-J. Comparison of the boundary-lubricating ability of bovine synovial fluid, lubricin, and Healon. J Biomed Mater Res. 1998; 40:414–418. [PubMed: 9570073]
29. Shuler, ML.; Kargi, F. Bioprocess Engineering: Basic Concepts. 2nd. Upper Saddle River, NJ: Prentice Hall PTR; 2002.
30. Zwietering MH, Jongenburger I, Rombouts FM, Vantriet K. Modeling of the bacterial-growth curve. Appl Environ Microbiol. 1990; 56:1875–1881. [PubMed: 16348228]
31. Abadian PN, Tandogan N, Jamieson JJ, Goluch ED. Using surface plasmon resonance imaging (SPRi) to study bacterial biofilms. Biomicrofluidics. 2014; 8:021804. [PubMed: 24753735]
32. Goluch, E.; Abadian, P.; Aninwene, GE., II; Webster, TJ. SPRi system for evaluating biomass accumulation and removal. USA patent. 61858181. 2013.
33. Abadian PN, Kelly CP, Goluch ED. Cellular analysis and detection using surface plasmon resonance (SPR) techniques. Anal Chem. 201410.1021/ac500135s
34. Puckett SD, Lee PP, Ciombor DM, Aaron RK, Webster TJ. Nanotextured titanium surfaces for enhancing skin growth on transcutaneous osseointegrated devices. Acta Biomater. 2009; 6:2352–2362. [PubMed: 20005310]
35. Chang DP, Abu-Lail NI, Guilak F, Jay GD, Zauscher S. Conformational mechanics, adsorption, and normal force interactions of lubricin and hyaluronic acid on model surfaces. Langmuir. 2008; 24:1183–1193. [PubMed: 18181652]
36. Swann DA, Slayter HS, Silver FH. The molecular structure of lubricating glycoprotein-I, the boundary lubricant for articular cartilage. J Biol Chem. 1981; 256:5921–5925. [PubMed: 7240180]
37. Elsaid KA, Machan JT, Waller K, Fleming BC, Jay GD. The impact of anterior cruciate ligament injury on lubricin metabolism and the effect of inhibiting tumor necrosis factor a on chondroprotection in an animal model. Arthritis Rheum. 2009; 60:2997–3006. [PubMed: 19790069]
38. Blewis ME, Nugent-Derfus GE, Schmidt TA, Schumacher BL, Sah RL. A model of synovial fluid lubricant composition in normal and injured joints. Eur Cells Mater. 2007; 13:26–38.
39. Jay GD, Harris DA, Cha C-J. Boundary lubrication by lubricin is mediated by O-linked β(1–3)Gal-GalNAc oligosaccharides. Glycoconjugate J. 2001; 18:807–815.
40. Coles JM, Chang DP, Zauscher S. Molecular mechanisms of aqueous boundary lubrication by mucinous glycoproteins. Curr Opin Colloid Interface Sci. 2010; 15:406–416.
41. Chang DP, Abu-Lail NI, Guilak F, Jay GD, Zauscher S. Conformational mechanics, adsorption, and normal force interactions of lubricin and hyaluronic acid on model surfaces. Langmuir. 2008; 24:1183–1193. [PubMed: 18181652]
42. Noyori K, Jasin HE. Inhibition of human fibroblast adhesion by cartilage surface proteoglycans. Arthritis Rheum. 1994; 37:1656–1663. [PubMed: 7980677]
43. Shi L, Ardehali R, Caldwell KD, Valint P. Mucin coating on polymeric material surfaces to suppress bacterial adhesion. Colloids Surf B: Biointerfaces. 2000; 17:229–239.
44. Jiang W, Woitach J, Keil R, Bhavanandan V. Bovine submaxillary mucin contains multiple domains and tandemly repeated non-identical sequences. Biochem J. 1998; 331:193–199. [PubMed: 9512479]
45. Jiang WP, Gupta D, Gallagher D, Davis S, Bhavanandan VP. The central domain of bovine submaxillary mucin consists of over 50 tandem repeats of 329 amino acids—Chromosomal localization of the BSM1 gene and relations to ovine and porcine counterparts. Eur J Biochem. 2000; 267:2208–2217. [PubMed: 10759843]

46. Schvartz I, Seger D, Shaltiel S. Vitronectin. Int J Biochem Cell Biol. 1999; 31:539–544. [PubMed: 10399314]

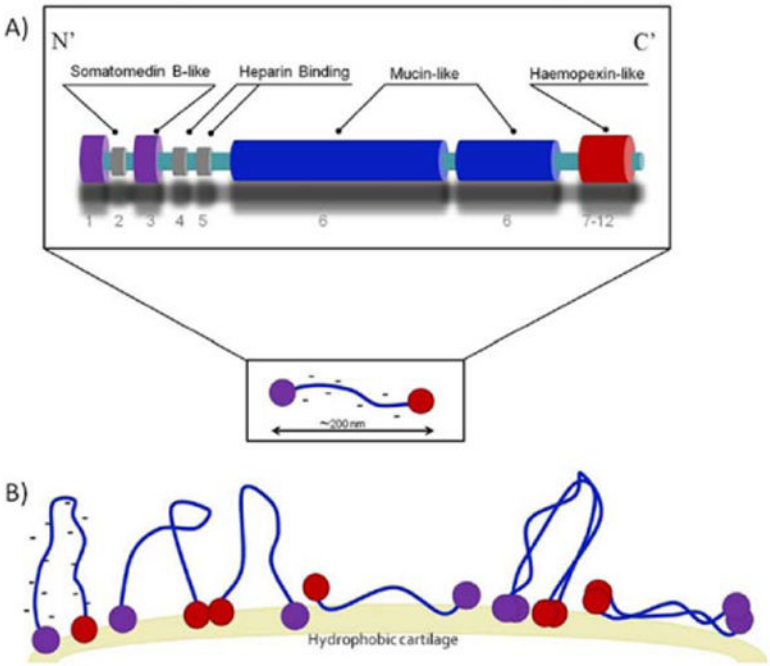

FIGURE 1.

Schematic representations of the structure of lubricin.[21–23] (A) A Mucin-like domain is found in the center and vitronectin like domains [analogues to SMB (somatomedin B) and PEX (hemopexin)] are found at the ends.[21,22] Lubricin is similar to vitronectin but it contains a negatively charged mucin domain. Lubricin may exist as a monomer or form dimers through disulfide bonds of the cysteine groups found in the globular tail regions. (B) Lubricin covers surfaces with end-grafted brushes.[24] Hydrophobic domains orient themselves toward hydrophobic surfaces and lubricin may form a loop structure with its mucin domain.[24] A LUB coating imparts a negatively charged hydrophilic nature on to the coated surface. [Color figure can be viewed in the online issue, which is available at wileyonlinelibrary. com.]

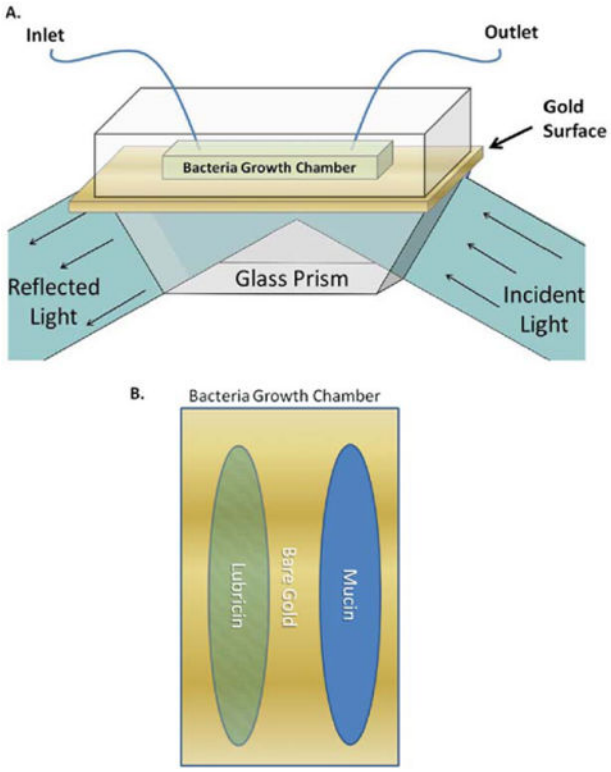

FIGURE 2.

(A) SPRi schematic: the growth chamber was treated with protein coatings, then seeded with bacteria. Fresh sterile LB growth media was pumped through the growth chamber. Light was projected through glass onto the gold-coated surface. A charge coupled device (CCD) camera was used to detect shifts in the intensity of light that exited the prism. (B) Bacterial growth chamber: lubricin and bovine submaxillary mucin were streaked in the bacteria growth chamber prior to bacterial seeding. [Color figure can be viewed in the online issue, which is available at wileyonlinelibrary.com.]

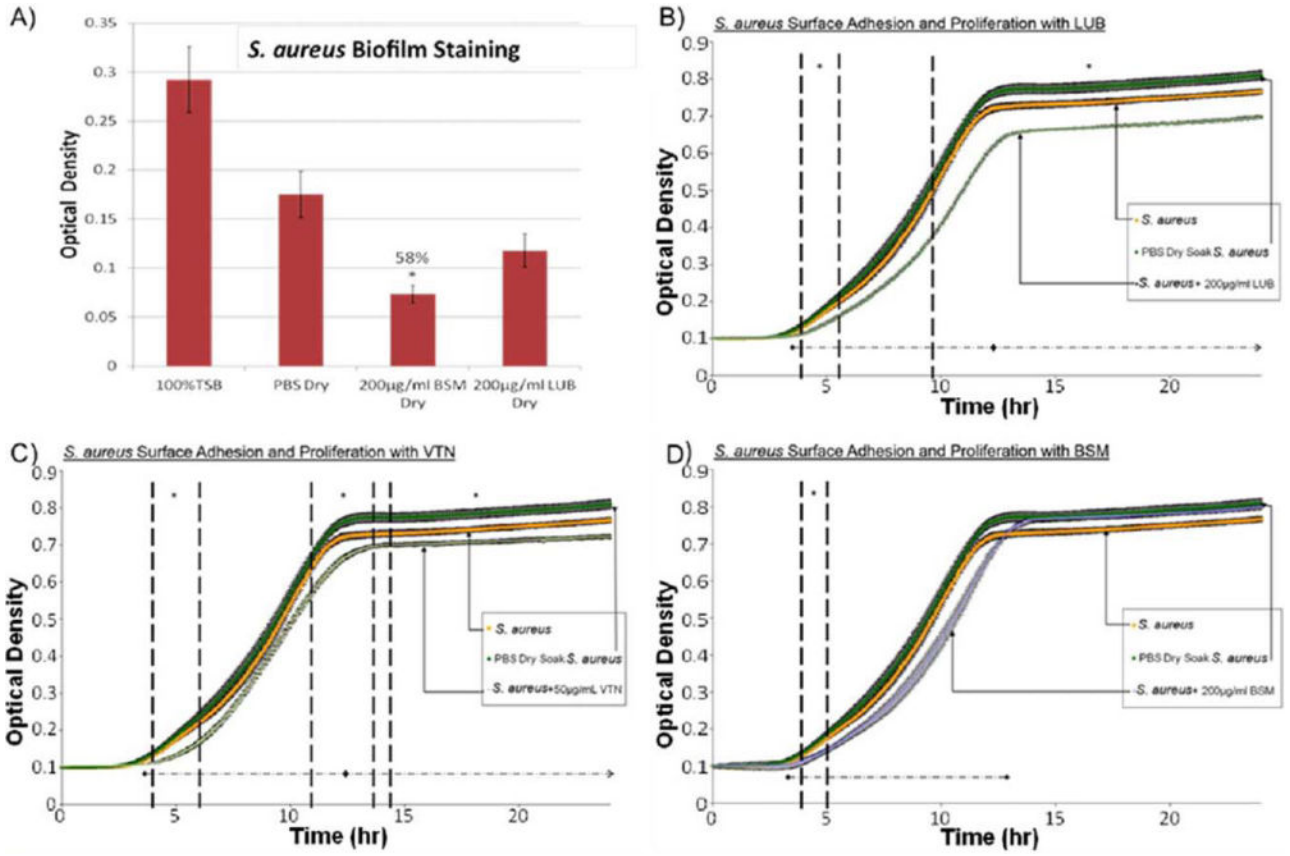

FIGURE 3.

(A) Crystal violet results after a 24 h S. *aureus* surface adhesion and proliferation trial. BSM-treated samples showed significant reduction in biofilm formation. Approximately 58% less biofilm was measured on BSM coated samples versus PBS-treated samples. (B) *S. aureus* surface adhesion and proliferation with LUB (200 µg/mL) over 24 h determined by optical density readings. LUB treatment significantly suppressed bacterial growth over the course of 24 h by 13.9%. Data = mean ± SEM; $N = 3$ (at 24 h $p < 0.01$). (C) *S. aureus* surface adhesion and proliferation with VTN (50 µg/mL) over 24 h determined by optical density readings. VTN treatment significantly suppressed bacterial growth over the course of 24 hrs by 11%. Data = mean ± SEM; $N = 3$ (at 24 h $p < 0.03$). (D) *S. aureus* surface adhesion and proliferation with BSM (200 µg/mL) over 24 h determined by optical density readings. Some significant reduction in proliferation was seen between 4.2 and 4.9 h time points. Data = mean ± SEM; $N = 3$ [*indicates areas of significant difference between protein-treated trials and PBS-treated trials] as determined by $p < 0.05$; ◆ indicates areas where using a confidence interval of 95% a significance reduction was seen between protein-treated trials and PBS-treated trials]. [Color figure can be viewed in the online issue, which is available at wileyonlinelibrary.com.]

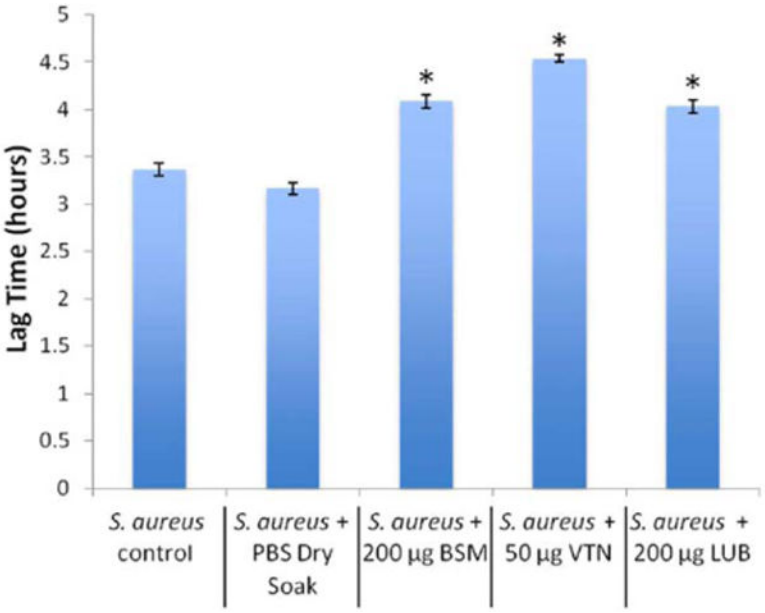

FIGURE 4.

Lag times for *S. aureus* with each protein derived from the mathematical model (data = ±95% confidence interval). *indicates significant difference from control and PBS dry soak ($p < 0.05$). [Color figure can be viewed in the online issue, which is available at wileyonlinelibrary.com.]

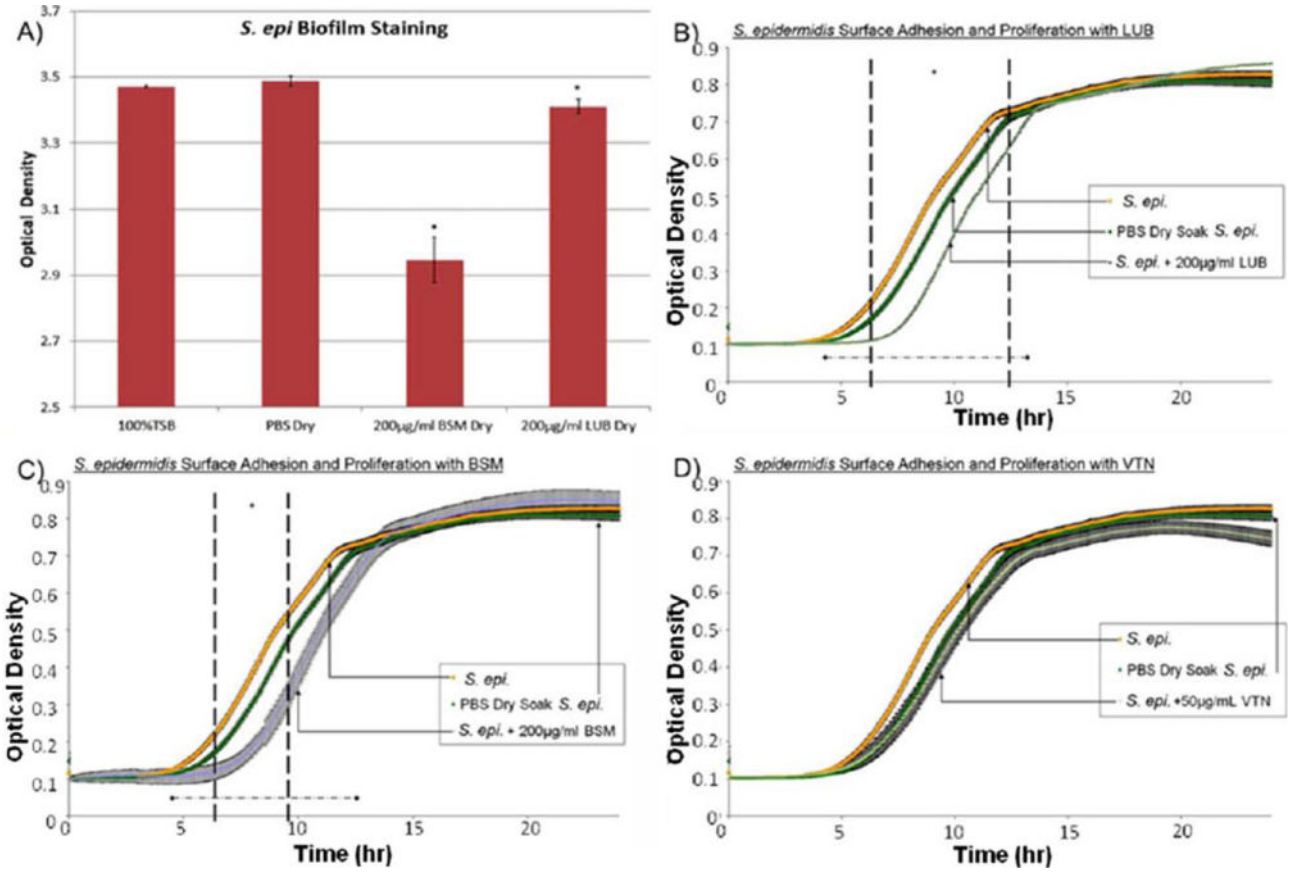

FIGURE 5.

(A) Crystal violet results after a 24 h *S. epidermidis* surface adhesion and proliferation trial. BSM-treated samples showed significant reduction in biofilm formation. Approximately 15.5% less biofilm was measured on BSM coated samples versus PBS-treated samples. (B) *S. epidermidis* surface adhesion and proliferation with LUB (200 µg/mL) over 24 h determined by optical density readings. LUB treatment significantly suppressed bacterial growth from 6.2 to 12.3 h time points ($p < 0.05$). Data = mean ± SEM; $N = 4$. (C) *S. epidermidis* adhesion and proliferation with BSM (200 µg/mL) over 24 h determined by optical density readings. Some significant reduction in proliferation seen between 6.3 and 9.6 h time points. Data = mean ± SEM; $N = 4$. (D) *S. epidermidis* surface adhesion and proliferation with VTN (50 µg/mL) over 24 h determined by optical density readings. VTN did not appear to significantly decrease bacterial proliferation. Although t-test indicated a significant decrease starting at 21.7 h this was not confirmed by the confidence interval calculations. Data = mean ± SEM; $N = 4$ [*indicates areas of significant difference between protein-treated trials and PBS-treated trials] as determined by $p < 0.05$; ◆ indicates areas where using a confidence interval of 95% a significance reduction was seen between protein-treated trials and PBS-treated trials]. [Color figure can be viewed in the online issue, which is available at wileyonlinelibrary.com.]

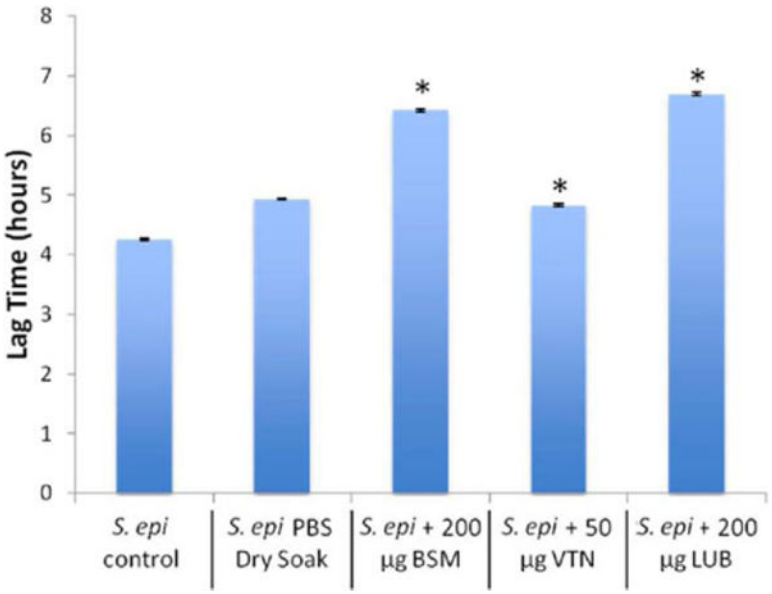

FIGURE 6.

Lag times for *S. epidermidis* with each protein derived from the mathematical model (data = ±95% confidence interval). *indicates significant difference from control and PBS dry soak ($p < 0.05$). [Color figure can be viewed in the online issue, which is available at wileyonlinelibrary.com.]

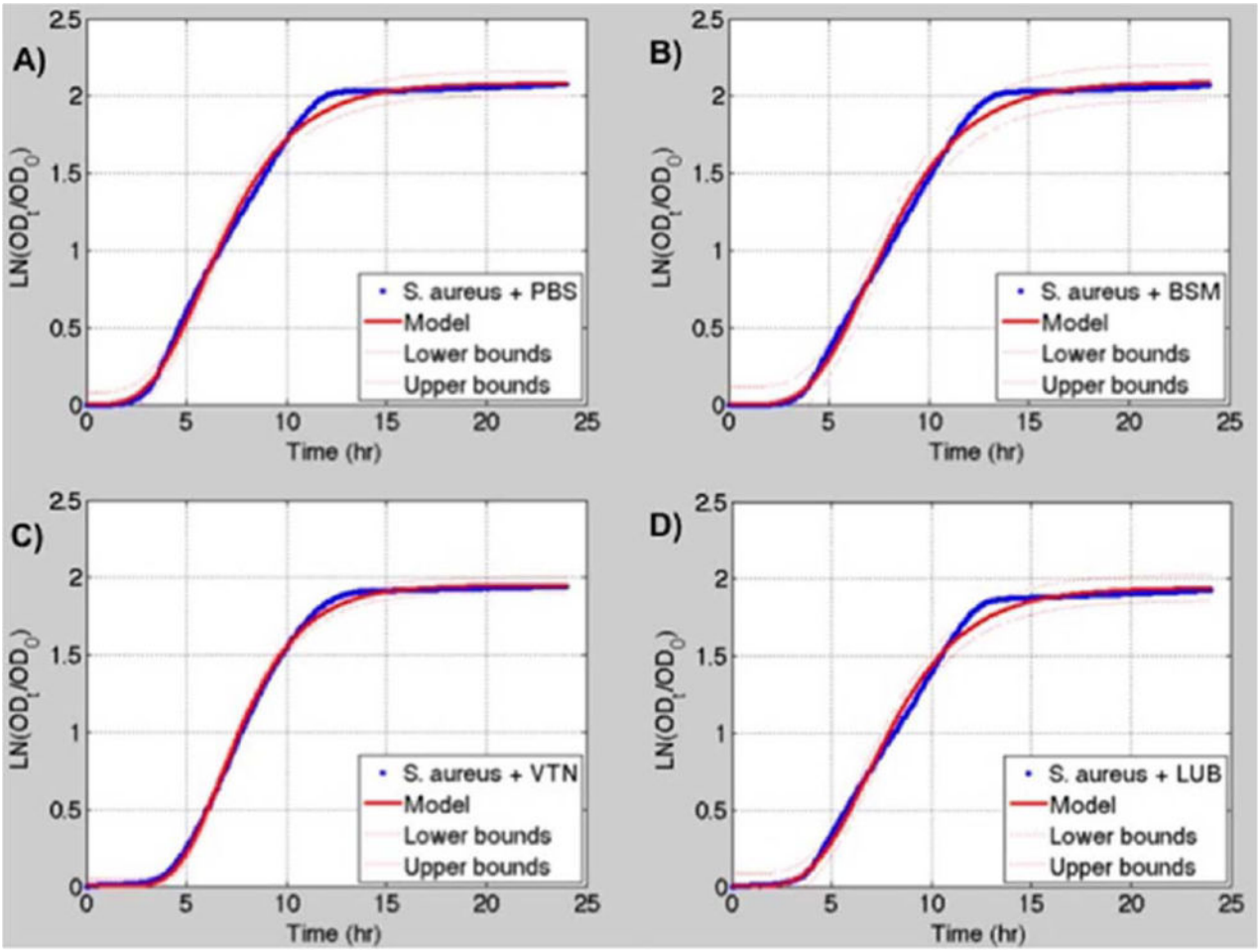

FIGURE 7.

(A) *S. aureus* + PBS growth data (blue) fitted to the modified Gompertz growth curve (red). (B) *S. aureus* + 200 μg/mL BSM growth data (blue) fitted to the modified Gompertz growth curve (red). (C) *S. aureus* + 50 μg/mL VTN growth data (blue) fitted to the modified Gompertz growth curve (red). (D) *S. aureus* + 200 μg/mL LUB growth data (blue) fitted to the modified Gompertz growth curve (red). 95% confidence interval for the models is shown by the dashed red lines. Logistic models are not shown. [Color figure can be viewed in the online issue, which is available at wileyonlinelibrary.com.]

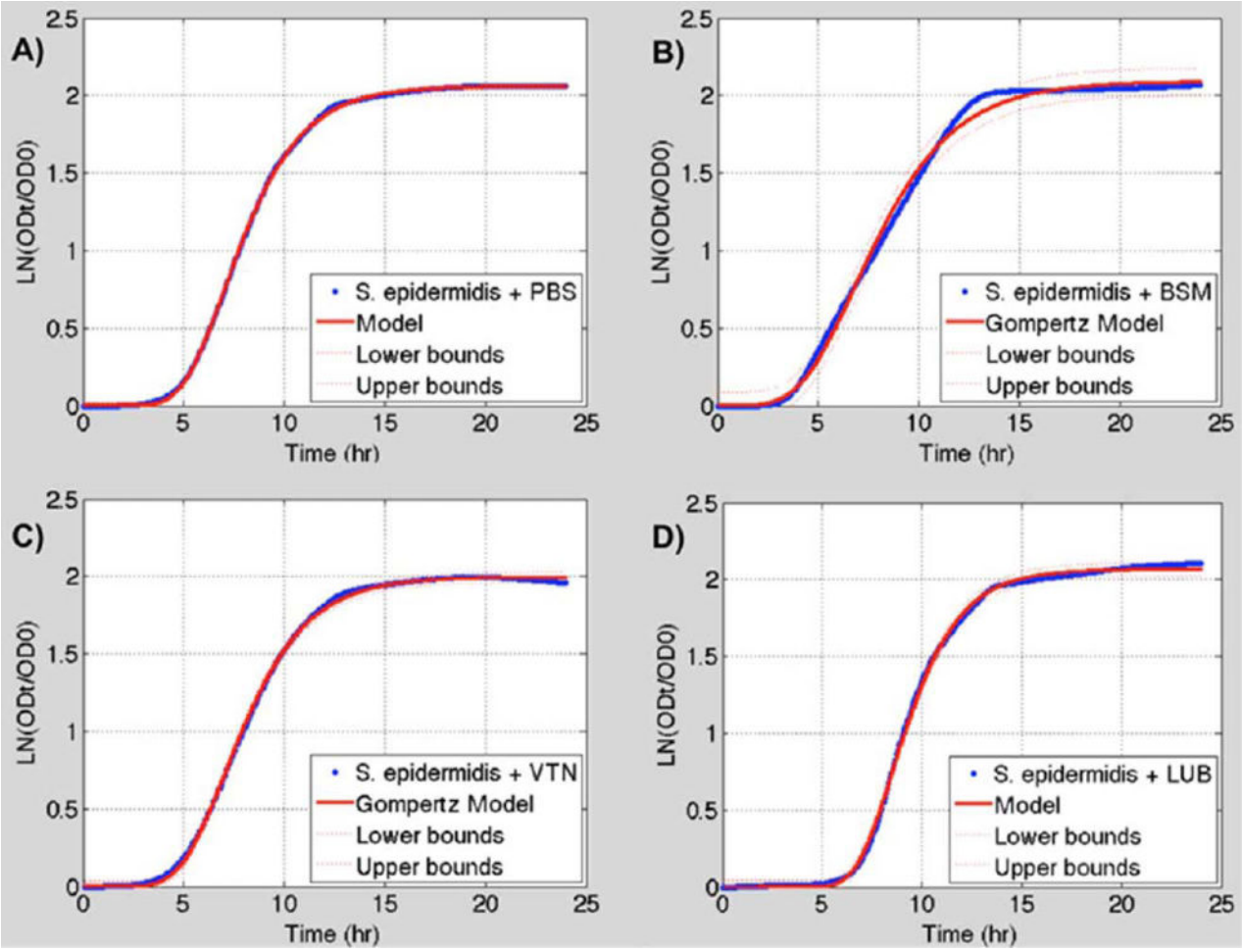

FIGURE 8.

(A) *S. epidermidis* + PBS growth data (blue) fitted to a modified Gompertz growth curve (red). (B) *S. epidermidis* + BSM growth data (blue) fitted to a modified Gompertz growth curve (red). (C) S. epidermidis + VTN growth data (blue) fitted to a modified Gompertz growth curve (red). (D) *S. epidermidis* + LUB growth data (blue) fitted to a modified Gompertz growth curve (red). 95% confidence interval for the models is shown by the dashed red lines. Logistic models are not shown. [Color figure can be viewed in the online issue, which is available at wileyonlinelibrary.com.]

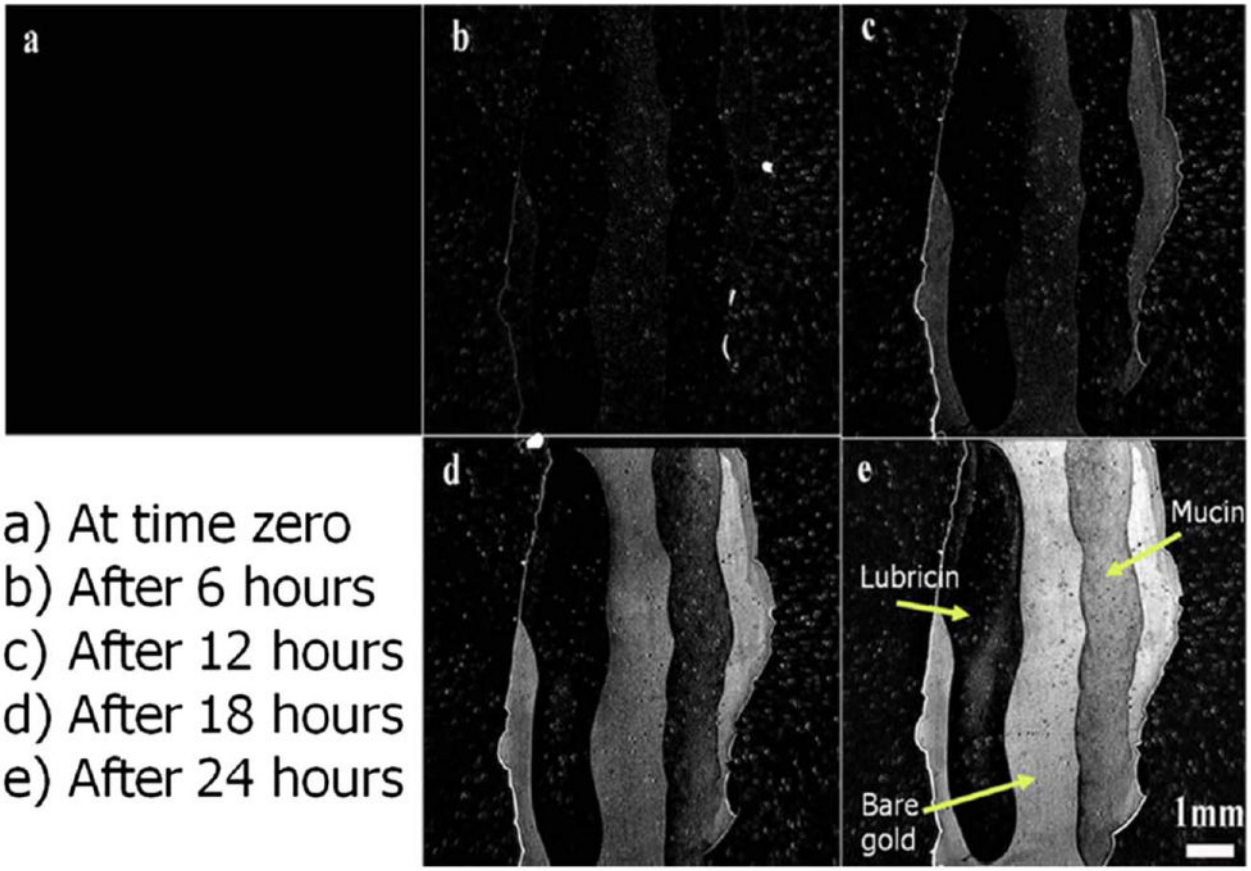

FIGURE 9.

SPRi images taken at time 0, 6, 12, 18, and 24 h time points: Lubricin coatings resulted in near complete blockage of biofilm adherence on the surface. [Color figure can be viewed in the online issue, which is available at wileyonlinelibrary.com.]

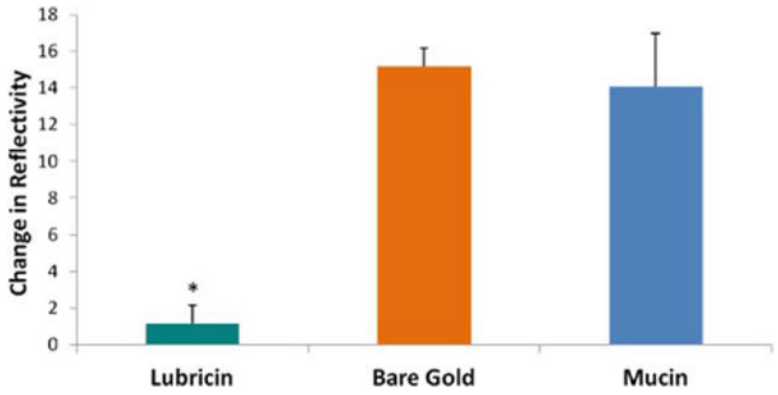

FIGURE 10.

SPRi change in reflectivity at the trial end point: lubricin showed over a 90% reduction of bacterial biofilm when compared to bare gold. Mucin only resulted in approximately 7% reduction. (Data = mean + SEM; $N = 3$; *indicates a significant difference between lubricin coated areas and both bare gold and mucin as determined by $p \ll 0.05$). [Color figure can be viewed in the online issue, which is available at wileyonlinelibrary.com.]

TABLE I

Summary of the Effect of Mucin, Vitronectin, and Lubricin on the Growth Curve Parameters of *S. aureus*

	Mucin	Vitronectin	Lubricin
Lag time (λ)	↓	↓	↓
Maximum specific growth rate (μ_m)	↓	↓	↓
Asymptote of growth	↓	↓	~

TABLE II

Summary of the Effects of Mucin, Vitronectin, and Lubricin on the Growth Curve Parameters of *S. epidermidis*

	Mucin	Vitronectin	Lubricin
Lag time (λ)	↓	↓	↓
Maximum specific growth rate (μ_m)	↓	↓	↓
Asymptote of growth	↓	↓	~

TABLE III

Contact Angle Results for Uncoated Tissue Culture Polystyrene

Blank/Untreated PS	Contact Angle	STD Error
Water	55.0	1.37
Ethylene glycol	32.4	0.20
Glycerol	58.8	0.38

Polystyrene samples coated with PBS suspended proteins showed complete wetting and thus are not displayed.